Shock and Vibration 10 (2003) 283–300
IOS Press

Experiments on optimal vibration control of a flexible beam containing piezoelectric sensors and actuators

Gustavo L.C.M. Abreu, José F. Ribeiro and Valder Steffen, Jr*
Federal University of Uberlândia, School of Mechanical Engineering, P.O. Box 593, 38400-902, Uberl ândia-MG, Brazil

Received 1 November 2002
Revised 10 April 2003

Abstract. In this paper, a digital regulator is designed and experimentally implemented for a flexible beam type structure containing piezoelectric sensors and actuators by using optimal control design techniques. The controller consists of a linear quadratic regulator with a state estimator, namely a Kalman observer. The structure is a cantilever beam containing a set of sensor/actuator PVDF/PZT ceramic piezoelectric patches bonded to the beam surface at the optimal location obtained for the first three vibration modes. The equations of motion of the beam are developed by using the assumed modes technique for flexible structures in infinite-dimensional models. This paper uses a method of minimizing the effect of the removed higher order modes on the low frequency dynamics of the truncated model by adding a zero frequency term to the low order model of the system. A measure of the controllability and observability of the system based on the modal cost function for flexible structures containing piezoelectric elements (intelligent structures) is used. The observability and controllability measures are determined especially to guide the placement of sensors and actuators, respectively. The experimental and numerical transfer functions are adjusted by using an optimization procedure. Experimental results illustrate the optimal control design of a cantilever beam structure.

Keywords: Optimal control design, smart structures, optimal location for sensors/actuators

1. Introduction

A single piezoelectric element called a self-sensing actuator combines actuator and sensing capabilities for collocated control [1]. The use of piezoelectric actuator/sensor pairs has been widely used in many vibration control applications of flexible structures [2–4].

The French scientists Pierre and Paul-Jacques Curie discovered piezoelectricity in 1880. The piezoelectric effect is observed in many crystalline materials, which strain when exposed to a voltage and produce a voltage when strained. In other words, these materials are capable of transforming mechanical energy into electrical energy and vice versa. Piezoelectric actuators and sensors are bonded to flexible structures such as beams and plates, forming the so-called smart structures.

Different methodologies have been used for modeling smart structures, however the most promising technique is the finite element method, as first presented for piezo-mechanical systems by [5]. Later this formulation was extended for different structural elements. [6] studied the modeling of one-dimensional piezoelectric patches embedded into the body of beams and formulated the moment generated by a voltage applied to the piezoceramics. [7] presented a piezoelectric finite element approach aiming at applications devoted to distributed dynamic measurement and control of advanced structures. The assumed modes approach has been extensively used throughout the literature to model the dynamics of distributed systems such as flexible beams

*Corresponding author. Fax: +55 34 3239 4282; E-mail: vsteffen@mecanica.ufu.br.

ISSN 1070-9622/03/$8.00

and plates [8]. This approach is used in this paper for modeling the flexible beam.

In control design problems, one is often interested in designing a controller for a particular frequency range. In such situations, it is common practice to remove the modes that correspond to frequencies that lie out of the bandwidth of interest and keep only the modes that directly contribute to the low frequency dynamics of the system. [4] suggested that the effect of higher frequency modes on the low frequency dynamics of the system can be captured by adding a zero frequency term to the truncated model to account for the compliance of the ignored modes. In the present work, this approach is taken.

The optimal control design applied to smart structures has been studied in several papers by using different methodologies. [9] presented a control system test bed which is used for active vibration control of a plate by using piezoelectric actuators. In that work, the authors applied a localized hybrid fuzzy-PD controller. The gains of the fuzzy-PD controller were obtained by using genetic algorithm techniques. [10] designed an optimal multivariable feedback controller for the active vibration control of a dynamic system consisting of a linear elastic plate with piezoelectric sensors and actuators. That contribution used PD and LQG/LTR control methods. [11] presented a new approach for simultaneous optimization of the intelligent structure together with the control system for vibration suppression.

The choice of the actuator location is an important issue in the design of actively controlled structures. The actuators should be placed at the locations so that the desired modes are excited most effectively [6]. Various engineering applications using classical optimization and genetic algorithm schemes for the determination of optimal piezoelectric actuator placement have been reported. [12] worked with genetic algorithms to determine optimal actuator size and location for two piezoelectric actuators bonded to a cantilever beam. [13] used a discrete-continuous optimization technique to determine the position of the actuators along the flexible structure and to obtain the controller gains. In that work the goal was to minimize the control effort applied to a beam type structure.

In this paper, the measures of controllability and observability are based on the modal cost function or modal cost analysis, as proposed by [14]. Such measures are used to guide the placement of sensors and actuators in flexible piezo-actuated structures.

To evaluate the usefulness of the proposed method, a digital regulator applied to the active vibration control of a cantilever beam type test structure was designed. The results obtained confirmed the applicability of the above technique and the stability of the control algorithm used.

2. Electro-mechanical model of a beam containing piezoelectric sensors and actuators

In this section, a model for a piezoelectric laminate beam with an actuator-sensor pair is obtained by using modal analysis techniques.

Figure 1(a) shows a flexible structure with an attached piezoelectric actuator-sensor pair. The piezoelectric patch on the upper side of the beam is used as an actuator, while the film on the bottom side serves as a sensor. The voltage that is applied to the actuator patch is represented by $V_a(t)$ and the voltage that is induced to the sensor film is represented by $V_s(t)$ (see Fig. 1(b)).

Consider a homogeneous Euler-Bernoulli beam (dimensions: L_b, b_b, h_b) as shown in Figs 1(a)–(b). The piezoelectric actuator and sensor have dimensions of $(x_{a2}-x_{a1})\times b_a \times h_a$ and $(x_{s2}-x_{s1})\times b_s \times h_s$, respectively (see Fig. 1(b)). The beam transverse deflection at point x and time t is denoted by $w(x,t)$, assuming the beam as a one-dimensional system.

A model of the structure is obtained through a modal analysis procedure. This approach exacts the finding of a solution to the partial differential equation that describes the dynamics of the flexible structure:

$$\rho_b A_b \frac{\partial^2 w}{\partial t^2} + E_b I_b \frac{\partial^4 w}{\partial x^4} = q(x,t) \tag{1}$$

where ρ_b, A_b, E_b and I_b represent density, cross-sectional area, Young's modulus of elasticity, and moment of inertia about the neutral axis of the beam, respectively.

2.1. Actuator dynamics

The total distributed load $q(x,t)$ generated by the piezoelectric actuator when it is deformed is given by:

$$q(x,t) = M_{ax} \frac{\partial^2 R}{\partial x^2} \tag{2}$$

where R is the generalized location function expressed as a function of the Heaviside function (H) [15]:

$$R(x) = H(x-x_1) - H(x-x_2) \tag{2.1}$$

The bending moment acting on the beam (denoted by M_{ax}) is given by [16]:

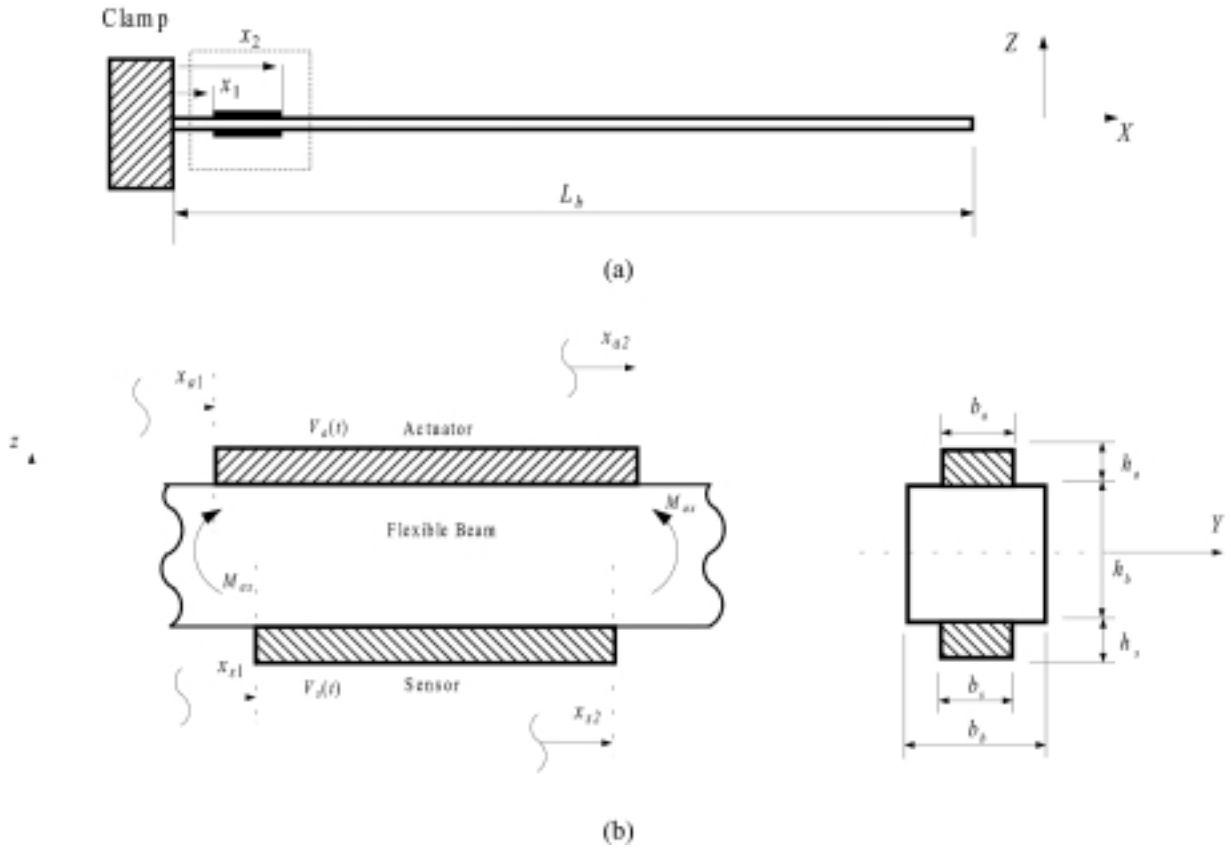

Fig. 1. (a) Flexible cantilever beam containing piezo-sensor and actuator and (b) Geometrical properties of the piezoelectric elements.

$$M_{ax} = \int_{h_b/2}^{h_b/2+h_a} \sigma_{ax}(x,t) b_a x dx \tag{3}$$

where:

$$\sigma_{ax} = E_a \varepsilon_{ax} \tag{3.1}$$

and

$$\varepsilon_{ax} = \frac{d_{31} V_a(t)}{h_a} \tag{3.2}$$

where d_{31} is the electric charge constant, E_a is the Young's modulus and h_a is the thickness of the PZT patch as shown in Fig. 1(b).

The evaluation of Eq. (3) through Eqs (3.1) and (3.2) gives the following expression:

$$M_{ax} = C_a V_a(t) \tag{4}$$

where C_a is a constant which depends on the geometry of the composite system:

$$C_a = \frac{1}{2} E_a d_{31} b_a (h_b + h_a) \tag{5}$$

The boundary conditions for the cantilever beam in Fig. 1(a) are:

$$\begin{aligned} &w(0,t) = 0 \\ &E_b I_b \frac{\partial w(0,t)}{\partial x} = 0 \\ &E_b I_b \frac{\partial^2 w(L_b,t)}{\partial x^2} = 0 \\ &E_b I_b \frac{\partial^3 w(L_b,t)}{\partial x^3} = 0 \end{aligned} \tag{6}$$

To use the assumed mode technique, the function $w(x,t)$ is expanded as an infinite series as follows [3]:

$$w(x,t) = \sum_{i=1}^{\infty} \phi_i(x) \eta_i(t) \tag{7}$$

where $\phi_i(x)$ are the eigenfunctions satisfying the ordinary differential equations resulting from the substitution of Eq. (7) into Eqs (1) and (6), and $\eta_i(t)$ are the temporal functions.

The mode shapes for clamped-free boundary conditions, Eq. (6), are assumed to be expressed as [17]:

$$\begin{aligned} \phi_i(x) = C_i [&\sin(\beta_i x) - \sinh(\beta_i x) \\ &+ \alpha_i (\cos(\beta_i x) - \cosh(\beta_i x))] \end{aligned} \tag{8}$$

where the following equations define α_i and β_i, respectively:

$$\alpha_i = \frac{\cos(\beta_i L_b) + \cosh(\beta_i L_b)}{\sin(\beta_i L_b) - \sinh(\beta_i L_b)} \tag{8.1}$$

$$1 + \cos(\beta_i L_b)\cos(\beta_i L_b) = 0 \tag{8.2}$$

and the constant C_i is determined by the condition expressed by the following expression:

$$\int_0^{L_b} \phi_i^2(x)dx = 1 \tag{9}$$

Substituting Eqs (7) and (2) into (1) yields:

$$\sum_{i=1}^{\infty} \begin{bmatrix} \rho_b A_b \phi_i(x)\ddot{\eta}_i(t) + \\ E_b I_b \phi_i^{''''}(x)\eta_i(t) \end{bmatrix} = M_{ax}\frac{\partial^2 R}{\partial x^2} \tag{10}$$

where (.) denotes time derivatives and ( ) represents space derivatives.

Pre-multiplying Eq. (10) by $\int_0^{L_b} \phi_i(x)dx$, the i-th equation, will be given by:

$$\begin{aligned} &\left(\rho_b A_b \int_0^{L_b} \phi_i^2(x)dx\right)\ddot{\eta}_i(t) \\ &+ \left(E_b I_b \int_0^{L_b} \phi_i(x)\phi_i^{''''}(x)dx\right)\eta_i(t) \\ &= M_{ax}\frac{\partial^2 R}{\partial x^2}\int_0^{L_b}\phi_i(x)dx \end{aligned} \tag{11}$$

Substituting Eqs (9) and (2.1) in Eq. (11), it is possible to obtain:

$$\begin{aligned} &\ddot{\eta}_i(t) + w_{ni}^2\eta_i(t) = \\ &k_a\lfloor\phi_i'(x_{a1}) - \phi_i'(x_{a2})\rfloor V_a(t) \end{aligned} \tag{12}$$

where:

$$\omega_{ni}^2 = \left(\frac{E_b I_b}{\rho_b A_b}\int_0^{L_b}\phi_i(x)\phi_x^{''''}(x)dx\right) \tag{12.1}$$

$$k_a = \frac{C_a}{\rho_b A_b} \tag{12.2}$$

The natural frequencies ω_{ni} are determined by using Eqs (12.1) and (8):

$$\omega_{ni}^2 = \frac{E_b I_b}{\rho_b A_b}\beta_i^4 \tag{12.3}$$

Modal damping (ζ_i) can be included in Eq. (12), as follows:

$$\begin{aligned} &\ddot{\eta}_i(t) + 2\zeta_i\omega_{ni}\dot{\eta}(t) + \omega_{ni}^2\eta_i(t) = \\ &k_a[\phi_i^{'}(x_{a1}) - \phi_i^{'}(x_{a2})]V_a(t) \end{aligned} \tag{13}$$

It is a very difficult task to determine modal structural damping by using physical principles. Therefore, ζ_i's are often estimated experimentally, which will be shown later in this paper.

Now, by taking the Laplace transform of Eq. (13), the transfer function of this system is obtained:

$$\frac{w(x,s)}{V_a(s)} = \sum_{i=1}^{\infty}\frac{k_a\phi_i(x)\lfloor\phi_i'(x_{a1}) - \phi_i'(x_{a2})\rfloor}{s^2 + 2\zeta_i\omega_{ni}s + \omega_{ni}^2} \tag{14}$$

This equation describes the elastic deflection of the flexible beam due to a voltage applied to the actuating piezoelectric.

2.2. Sensor dynamics

The net forcing of the beam is equivalent to two equal and opposite moments applied to the beam at the endpoints of the actuator, as shown in Fig. 2. Due to the piezoelectric effect, a strain-induced voltage appears in the sensors.

The electric charge distribution $q_s(t)$, i.e., the charge per unit area, is given by [18]:

$$q_s(x,t) = \frac{k_{31}^2}{g_{31}}\varepsilon_{sx}(x,t) \tag{15}$$

where k_{31} is the electromechanical coupling factor and g_{31} is the piezoelectric voltage constant in the X direction. Using Hooke's law for the beam deflection in the X direction (see Fig. 2), the expression for the strain in the sensor patch is obtained as [3]:

$$\varepsilon_{sx}(x,t) = -\left(\frac{h_b}{2} + h_s\right)\frac{\partial^2 w}{\partial x^2} \tag{16}$$

The total charge accumulated on the sensing layer can be found by integrating $q_s(x,t)$ over the entire length of the piezoelectric element [18]:

$$\begin{aligned} Q_s(t) &= \int_{x_{s1}}^{x_{s2}} b_s q_s(x,t)dx \\ &= -b_s\left(\frac{h_b}{2} + h_s\right)\frac{k_{31}^2}{g_{31}}\frac{\partial w(x,t)}{\partial x}\Big|_{x_{s1}}^{x_{s2}} \end{aligned} \tag{17}$$

Substituting Eq. (7) into (17), yields:

$$Q_s(t) = k_s\sum_{i=1}^{\infty}\eta_i(t)[\phi_i'(x_{s1}) - \phi_i'(x_{s2})] \tag{18}$$

where k_s is given by:

$$k_s = b_s\left(\frac{h_b}{2} + h_s\right)\frac{k_{31}^2}{g_{31}} \tag{19}$$

The piezoelectric sensor is similar to an electric capacitor and the voltage across the two layers is given

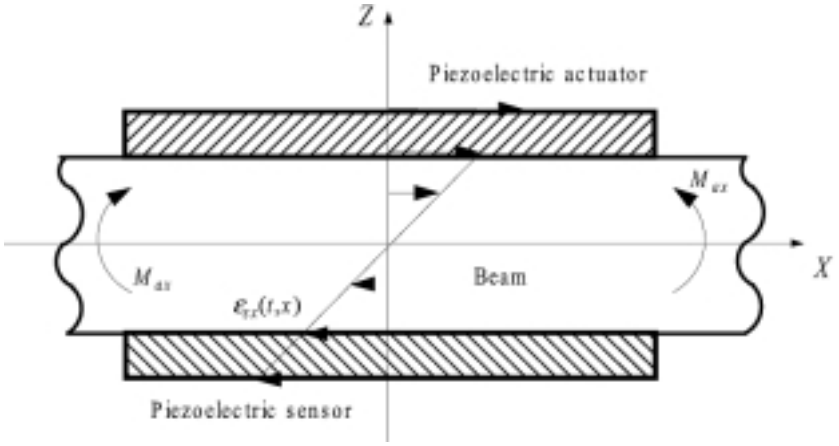

Fig. 2. Piezoelectric distributed sensor-actuator-beam configuration and associated strain distribution.

by the following formula:

$$V_s(t) = \frac{Q_s(t)}{C_s b_s(x_{s2} - x_{s1})} \tag{20}$$

where C_s is the capacitance per unit area of the piezoelectric sensor and $b_s(x_{s2} - x_{s1})$ is the surface area of the piezoelectric element.

If the piezo-sensor is connected to a voltage amplifier as depicted in Fig. 3, the sensor output voltage is [19]:

$$V_s(t) = \frac{Q_s(t)}{C_r} \tag{21}$$

where C_r stands for the circuit capacitance (see Fig. 3).

The circuit configuration shown in Fig. 3 was used in the present contribution. The corresponding parameters will be presented later on.

Substituting Eq. (18) in Eq. (21), yields:

$$V_s(t) = \frac{k_s}{C_r} \sum_{i=1}^{\infty} \eta_i(t)[\phi_i'(x_{s1}) - \phi_i'(x_{s2})] \tag{22}$$

Taking the Laplace transform of Eqs (22) and (13), the expression for $V_s(s)$ in terms of the input voltage $V_a(s)$ is obtained:

$$\frac{V_s(s)}{V_a(s)} = \tag{23}$$

$$\sum_{i=1}^{\infty} \frac{k_s k_a[\phi_i'(x_{s1}) - \phi_i'(x_{s2})][\phi_i'(x_{a1}) - \phi_i'(x_{a2})]}{C_r(s^2 + 2\zeta_i\omega_{ni}s + \omega_{ni}^2)}$$

This equation is the transfer function of the circuit, i.e., the relation between the voltage applied to the actuator and the voltage induced in the piezoelectric sensor.

3. Taking into account out of bandwidth modes

As an infinite number of modes are taken into account in the above formulation, Eqs (14) and (23) represent infinite-dimensional transfer functions.

In a typical control design scenario, the designer is often interested only in a particular bandwidth. Therefore, an approximate model of the system that best represents its dynamics in the prescribed frequency range is needed. A natural choice in this case is to simply ignore the modes which correspond to the frequencies that lie outside of the bandwidth of interest. Equation (23) is rewritten by limiting the number of modes considered to N.

$$\frac{V_s(s)}{V_a(s)} = G(s) = \sum_{i=1}^{N} \frac{F_i}{s^2 + 2\zeta_i\omega_{ni}s + \omega_{ni}^2} \tag{24}$$

where F_i is given by:

$$F_i = \frac{k_s k_a}{C_r}[\phi_i'(x_{s1}) - \phi_i'(x_{s2})] \\ [\phi_i'(x_{a1}) - \phi_i'(x_{a2})] \tag{24.1}$$

The drawback of this approach is that the truncated higher order modes may contribute to the low frequency dynamics in the form of distorting zero locations [20] suggests a way of dealing with this problem. The idea is to allow for a constant feed through term in Eq. (24) to account for the compliance of omitted higher order modes of Eq. (23). That is, to approximate Eq. (24) or $G(s)$ by:

$$\hat{G}(s) = G(s) + K_c \tag{25}$$

where K_c is a constant that considers the effect of dynamical responses of higher order modes.

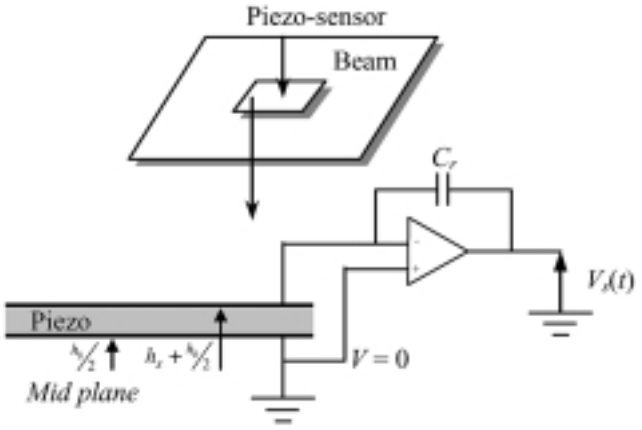

Fig. 3. Piezoelectric transducer charge amplifier.

[20] found the optimal value of K_c so that the effect of higher order modes on the low frequency dynamics is minimized in some measure. The optimal value of K_c was found to be:

$$K_c = \frac{1}{2\omega_c} \sum_{i=N+1}^{N_t} \frac{F_i}{\omega_i} \ln\left(\frac{\omega_i + \omega_c}{\omega_i - \omega_c}\right) \tag{26}$$

where ω_c represents the cut-off frequency chosen to lie within the interval: $\omega_c \in (\omega_N, \omega_{N+1})$.

In the experimental part of this paper, the above approach for a testbed cantilever beam type structure will be shown.

4. State space representation and controller design

Using Eq. (13) and the corrected model for Eq. (23), the state space model of the system is found to be:

$$\{\dot{q}(t)\} = [A]\{q(t)\} + [B]V_a(t) \tag{27}$$

$$V_s(t) = [C]\{q(t)\} + [D]V_a(t) \tag{28}$$

where:

$$\{q(t)\} = [\eta(t) \quad \dot{\eta}(t)]^T \tag{29.1}$$

$$[A] = \begin{bmatrix} 0 & I \\ -\omega_{ni}^2 & -2\zeta_i\omega_{ni} \end{bmatrix} \tag{29.2}$$

$$[B] = k_a * \begin{bmatrix} 0 \\ \phi_i'(x_{a1}) - \phi_i'(x_{a2}) \end{bmatrix} \tag{29.3}$$

$$[C] = \frac{k_s}{C_r} * [\phi_i'(x_{s1}) - \phi_i'(x_{s2}) \quad 0] \tag{29.4}$$

$$[D] = K_c \tag{29.5}$$

where I is the identity matrix, and k_a and k_s are the actuator and sensor constants defined by Eqs (12.2) and (19), respectively.

Since a digital computer is used to implement the proposed controller, it is necessary to discretize the continuous time system.

The state-space system given by Eqs (27) and (28) is used to design an optimal controller. The control algorithm used here is an iterative version of the Linear Quadratic Regulator (LQG). The goal is to find an optimal linear feedback controller while respecting a prescribed maximum voltage applied to the piezoelectric actuators to prevent their depoling. Hence, a full state feedback control is considered to minimize the cost function defined by Eq. (30) subject to the linear constraints Eq. (27) and to the voltage limitation $V_a < V_{a\max}$.

$$J = \int_0^\infty [\{q\}^T Q\{q\} + \{V_a\}^T R\{V_a\}]dt \tag{30}$$

Evidently, the performance of this controller depends on the state Q and input R weight matrices, where Q defines the relative weight of each state variable and R stands for the relative weight of each actuator voltage. The latter is supposed to be in the form $R = \gamma I$ and the factor γ is then adjusted automatically to limit the maximum voltage, through an iterative algorithm. Consequently, the control gain matrix $[G_c]$ is evaluated, for each value of γ, by solving the algebraic Riccati equation [21]. For the linear feedback of the controlled modes, the control law is:

$$\{V_a\} = -[G_c]\{q\} = -(\lfloor G_p \rfloor \; [G_d])\{q\} \tag{31}$$

where $[G_c]$ is the feedback gain matrix, and $[G_p]$ and $[G_d]$ are the displacement and velocity parts of $[G_c]$, respectively.

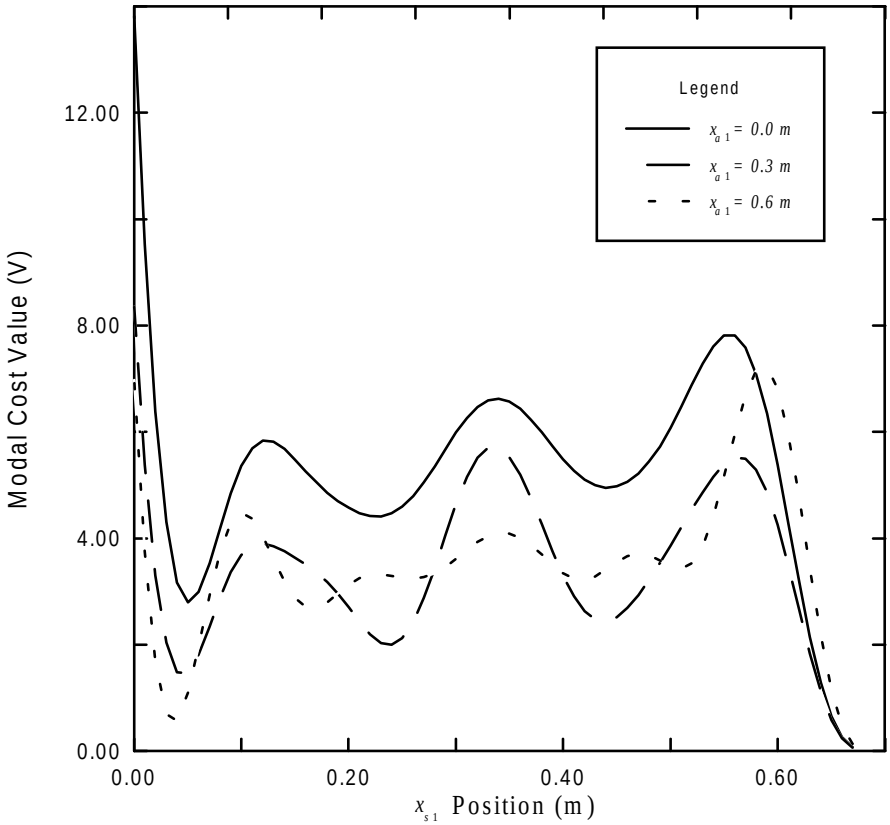

Fig. 4. Modal cost (V) versus sensor and actuator locations.

However, the control law cannot be implemented since all the states are not usually available. So a dynamic observer to estimate the states was designed [21]:

$$\{\dot{\hat{q}}\} = ([A] - [L][C])\{\hat{q}\} + ([B] + [L][D])\{V_a\} + [L]\{V_s\} \tag{32}$$

where $[L]$ is the observer gain.

The dynamic observer gain $[L]$ is obtained by solving an algebraic Riccati equation corresponding to the assumed state noise covariance matrix Q_e and measurement noise matrix R_e (see Eq. (30)). Since the system is observable, the gain matrix $[L]$ is calculated by using pole placement techniques. The location of the estimator poles should be carefully chosen so that fast convergence of the estimated states to the actual states is achieved. In doing this, the observer should not be very sensitive to noise (that may accompany the sensor signals).

Substituting Eq. (31) into (32), yields:

$$\{\dot{\hat{q}}\} = ([A] - [L][C] - [B][G_c] + [L][D][G_c])\{\hat{q}\} + [L]\{V_s\} \tag{33}$$

where the control law is:

$$\{V_a\} = -[G_c]\{\hat{q}\} \tag{34}$$

5. Modal cost function

In this section the problem of choosing the optimum locations for the piezoelectric elements used in the active vibration control of the structure is discussed. For this purpose, modal cost techniques will be used, i.e., how the controllability/obsevability of the system is changed as the piezoelectric actuators/sensors move along the structure [14].

Assuming the pair (A, B) controllable and (A, C) observable (see Eqs (29.2) to (29.4)), the controllability and observability are measured according to the grammians, as defined in the following equations [22]:

$$W_c(0, t_f) = \int_0^{t_f} e^{A\tau} B B^{\tau} e^{A^T \tau} d\tau \tag{35.1}$$

$$W_c(0, t_f) = \int_0^{t_f} e^{A^T \tau} C^{\tau} C e^{A\tau} d\tau \tag{35.2}$$

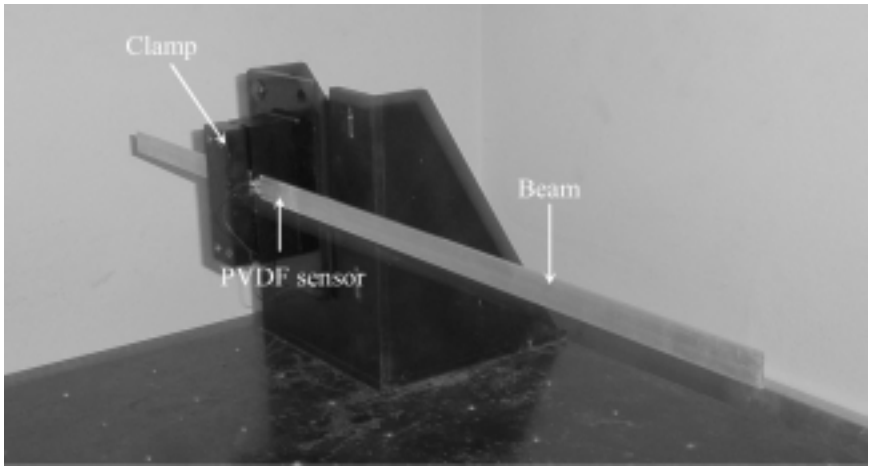

Fig. 5. Experimental apparatus.

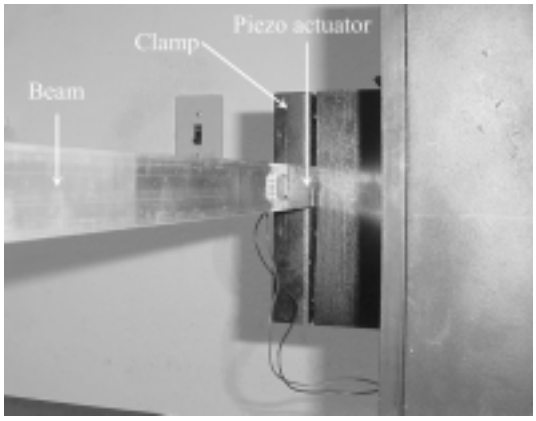

Fig. 6. Piezoelectric actuator location.

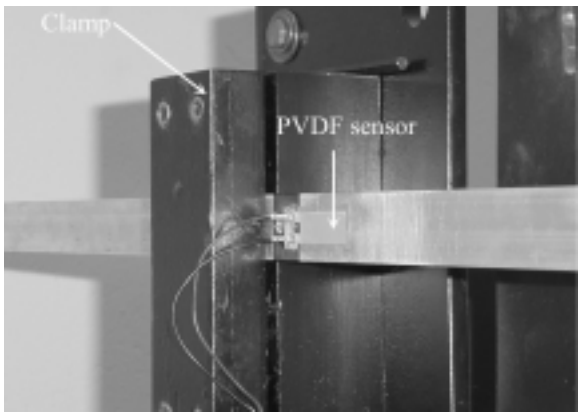

Fig. 7. Piezoelectric sensor location.

where t_f is some fixed final time and W_c and W_o satisfy the algebraic Lyapunov equations:

$$W_c A^T + A W_c + B B^T = 0 \tag{35.3}$$

$$A^T W_o + W_o A + C^T C = 0 \tag{35.4}$$

[23] suggested a measure of the effect of the actuators/sensors positions in the dynamical system by using a quadratic cost function:

$$V = \sum_{i=1}^{m} \int_0^\infty y^{iT}(t) Q_c y^i(t) dt \tag{35.5}$$

where the vector $y^i(t)$ is composed of output variables x^i due to impulsive inputs $u_i(t) = \delta(t)$ (with $u_j(t) = 0,\ i \neq j$), applied at $t = 0$, with zero initial conditions, and Q_c is a weight matrix.

Substituting the relation:

$$y^i(t) = C x^i(t) \tag{35.6}$$

into Eq. (35.5), yields:

$$V = \sum_{i=1}^{m} \int_0^\infty x^{iT}(t) C^T Q_c C x^i(t) dt \tag{35.7}$$

The unit impulse response for zero initial condition in the ith-direction is given by [24]:

$$x^i(t) = e^{At} x(0) + \int_0^t e^{A(t-\tau)} B u_i(\tau) d\tau \tag{35.8}$$

Considering zero initial conditions, Eq. (35.8) is given by:

$$x^i(t) = e^{At} B \tag{36}$$

Substituting Eq. (36) into (35.7), yields:

$$V = Q_c C \left[\sum_{i=1}^{m} \int_0^\infty e^{At} B B^T e^{A^T t} dt \right] C^T \tag{37}$$

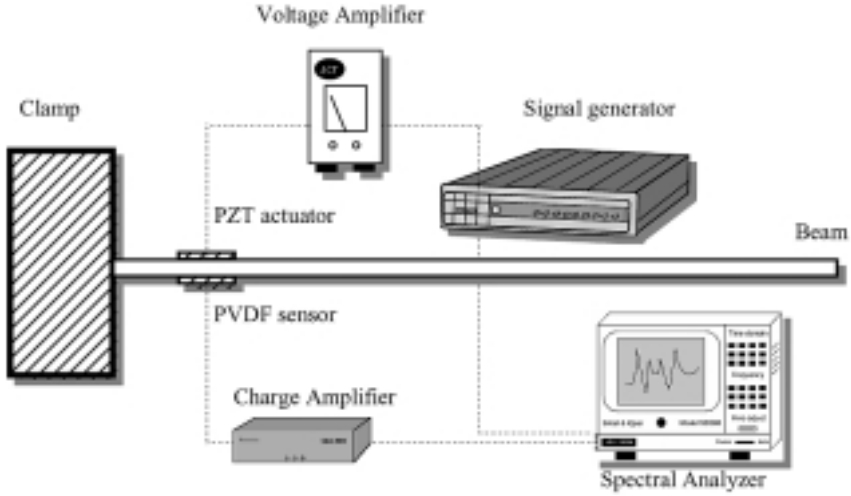

Fig. 8. Scheme of the experimental setup for system model identification.

Table 1
Characteristics of the piezo-structure

Properties	Units	Piezoelectric		Beam
		Sensor	Actuator	
E (Young's modulus)	Gpa	4	55	69
ρ (density)	Kg/m^3	1780	7700	2690
d_{31} (Charge constant)	C/m^2/(N/m^2)	23×10^{-12}	-179×10^{-12}	–
g_{31} (Voltage constant)	V/m/(N/m^2)	216×10^{-3}	10×10^{-3}	–
k_{31} (coupling coef.)	–	0.12	0.30	–
b (width)	m $\times 10^{-3}$	12	21	25.8
h (thickness)	m $\times 10^{-3}$	0.2	0.254	3.4
L (Length)	m $\times 10^{-3}$	30	45	700

Substituting Eq. (35.1) into (37), the cost function V is derived as follows:

$$V = \text{trace}\{Q_c C W_c C^T\} \tag{38}$$

where trace{ } denotes the trace (diagonal sum) of the matrix { }.

If the cost function (V) of a particular sensor/actuator location is zero, the sensor/actuator has no authority over those modes. On the other hand, if a given sensor/actuator location has a maximum cost value, the actuator/sensor has maximum authority over those modes.

Based on these principles it is possible [23]:

- to compare different sensor and actuator configurations and to choose the one that contributes the most to the cost function, and,
- to analyze the importance of the contribution of a given sensor/actuator in the cost function V with respect to the others.

6. Optimal placement of piezo sensors and actuators by using the modal cost function

In order to test the proposed optimization method to find the optimal placement of sensors and actuators, a cantilever aluminium beam type structure containing one set of sensor/actuator PVDF/PZT ceramic piezoelectric elements bonded to the beam surface is considered. The characteristics of the resulting mechatronic structure is shown in Table 1.

The main purpose of this section is to find the optimal placement of sensors (x_{s1}, x_{s2}) and actuators (x_{a1}, x_{a2}) bonded to the upper and bottom surfaces of the beam.

The output observability/controllability, that is the participation of each sensor/actuator in the output cost function is computed by using Eq. (38). It means that the configuration presenting the largest cost function index is the one whose output is the largest.

The computed output (Eq. (38)) of the system for different placements of the sensor (x_{s1}) and actuator (x_{a1}) are summarized in Fig. 4, where the weight matrix

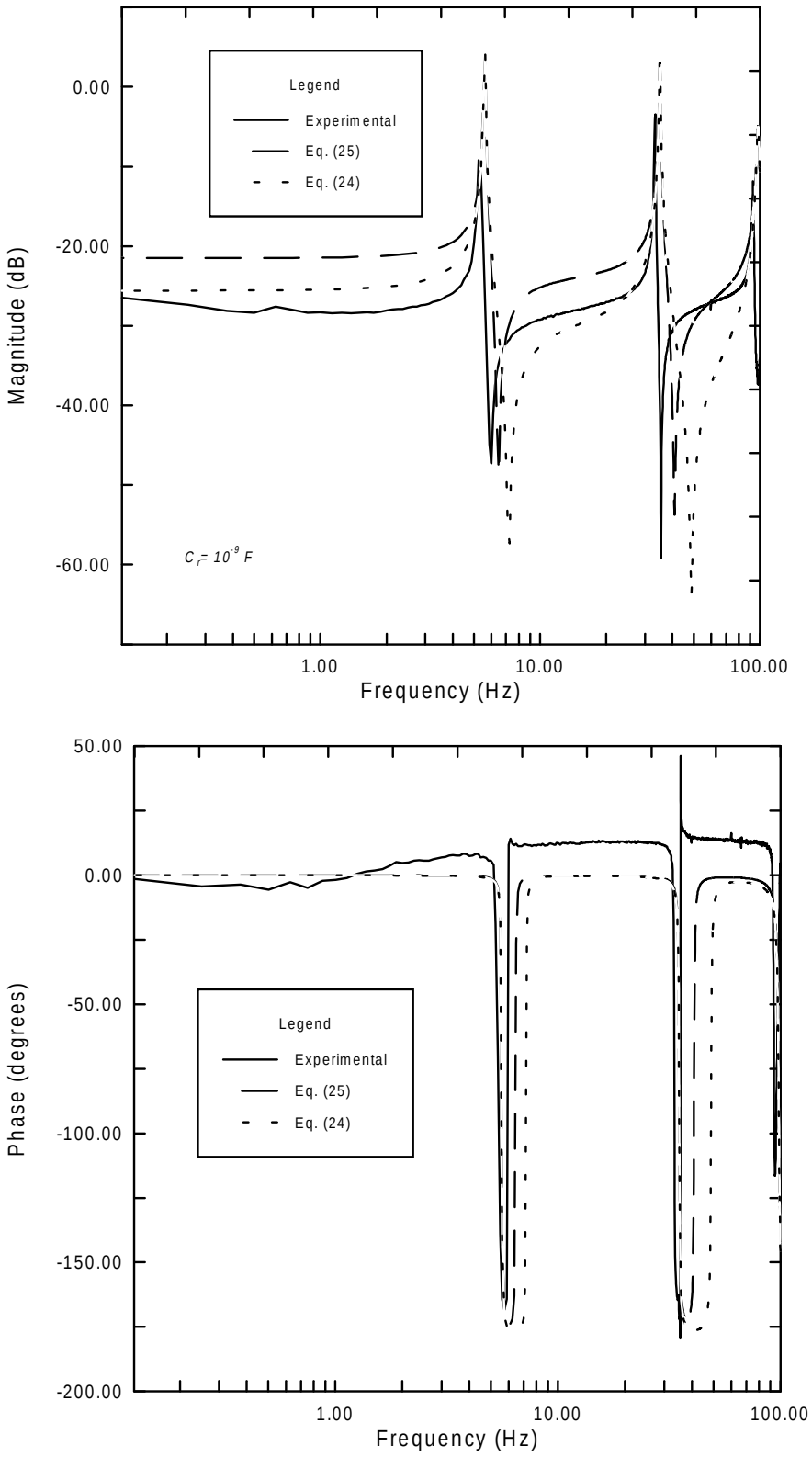

Fig. 9. Experimental and numerical transfer functions.

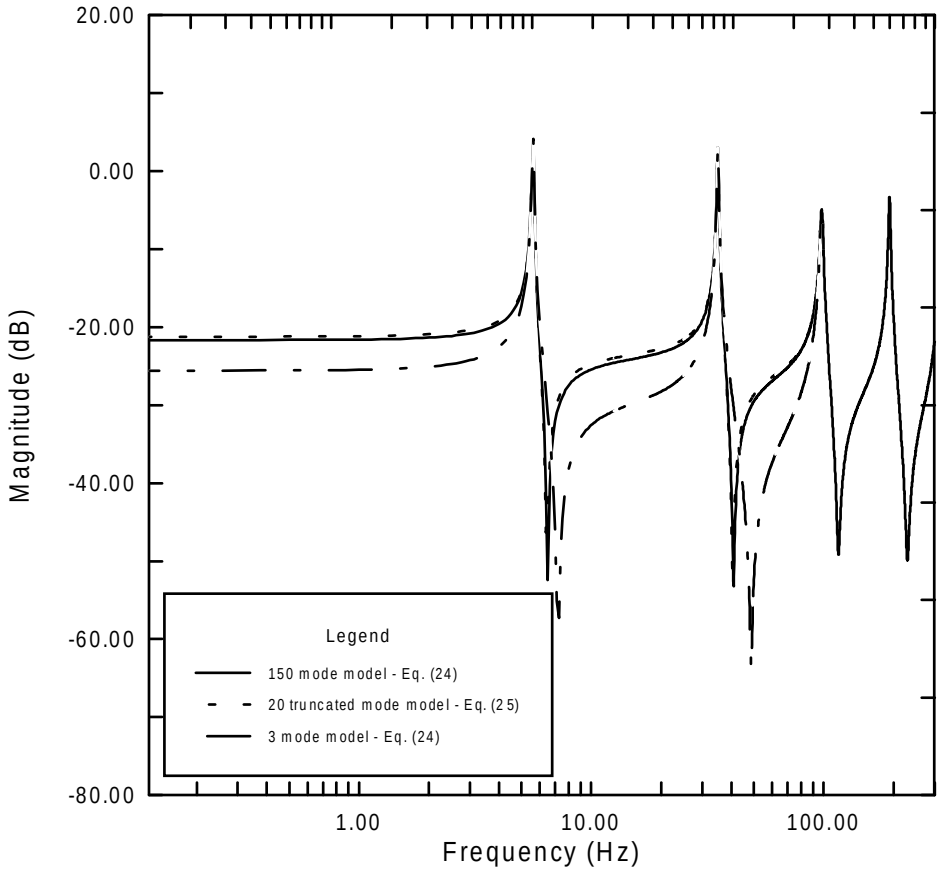

Fig. 10. Comparison of the transfer functions of the 150 mode model, 20 truncated mode model, and the 3 mode model of the flexible beam.

$Q_c = I$ (identity matrix). Matrices A, B and C are given by Eqs (29.2), (29.3), and (29.4), respectively, $C_r = 10^{-9}F$ and the number of modes (Eq. 24) is $N = 20$. The x_{s2} and x_{a2} values are obtained by using the following relations:

$$x_{s2} = L_s + x_{s1} \tag{39}$$

$$x_{a2} = L_a + x_{a1} \tag{40}$$

where L_s and L_a are the sensor and actuator lengths as given in Table 1.

As can be seen in Fig. 4, the magnitude of the modal cost function V for the sensor and actuator locations given by $x_{s1} = 0.0m$; $x_{a1} = 0.0m$, is larger than those of the remaining locations. This result confirms that the selected configuration should require less control energy, and therefore, the associated optimal controller design will entail smaller gain values in matrices $[G_p]$ and $[G_d]$.

7. Correlation of numerical and experimental results for the system transfer function

To validate the methodology presented in the previous sections, an experimental apparatus was constructed (see Fig. 5). It is constituted by a flexible cantilever aluminium beam structure with piezoelectric sensor and actuator elements symmetrically bonded to both sides of the beam. The characteristics of the experimental model (dimensions and material properties) are listed in Table 1.

The PZT actuator patch [25] (model QP10N) and PVDF sensor film were attached to the beam by using the optimal placement results as obtained in Section 6 (see Figs 6 and 7).

In the scheme of the experimental setup presented in Fig. 8, a signal generator was used to produce a bandwidth noise signal (0–100 Hz) applied to the voltage amplifier [25] (model 1224/5). The actuator [25] (model QP10N) is excited by the voltage amplifier and the structural vibrations are measured by using the

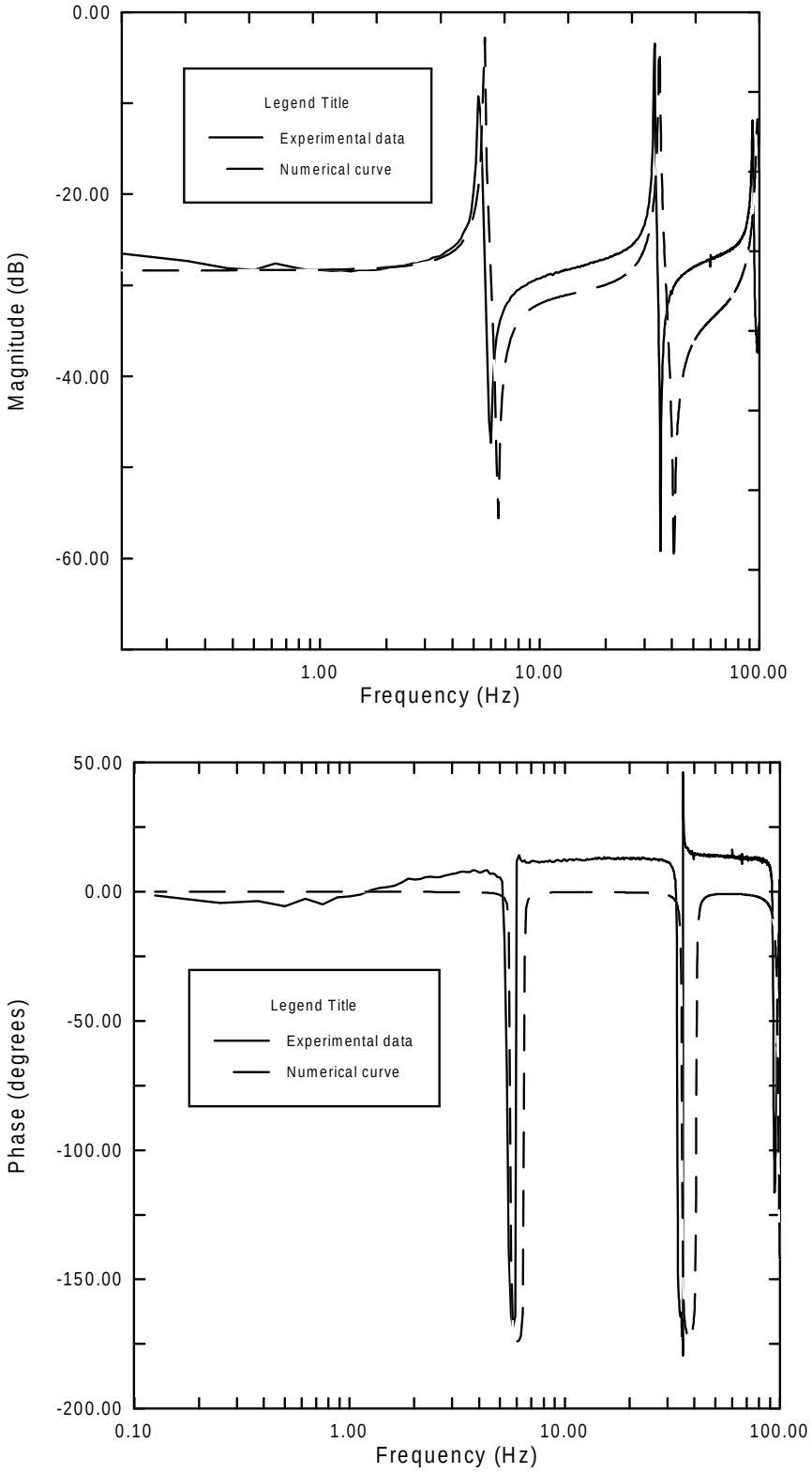

Fig. 11. Experimental and adjusted model transfer functions.

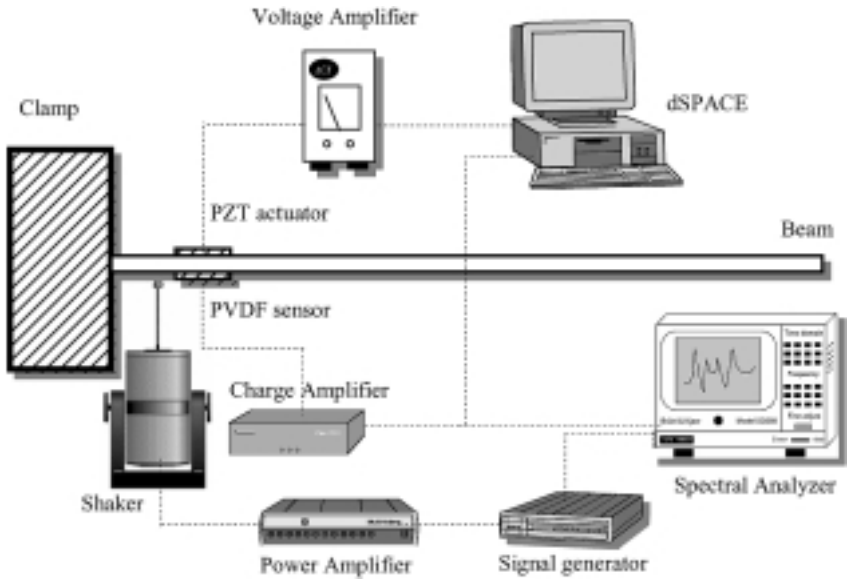

Fig. 12. Scheme of the vibration control experiment.

Table 2
First three modes of the cantilever beam

Mode i	Numerical ω_i (Hz)	Experimental ω_i (Hz)	Damping $\zeta_i \times 10^{-3}$
1	5.59	5.25	3.88
2	35.07	33.37	5.83
3	98.21	93.11	12.56

PVDF sensor film. In this experiment, a Spectral Analyzer (Scientific Atlanta – model SD380) is used to determine the frequency response of the beam.

The numerical (Eqs (24) and (25)), and experimental diagrams for the transfer functions are shown in Fig. 9.

The first three simulated (Eq. (12.3)) and experimentally obtained frequencies and modal dampings [26] are shown in Table 2.

Figure 9 presents the transfer function of the piezo-beam, by taking into account the first three modes of the beam (Eq. (24)). The remaining twenty modes are calculated through Eq. (26) and their influence is added to the reduced transfer function according to Eq. (25). The above described situation is compared with two other cases, namely: 1 – the transfer function is obtained by using Eq. (24) ($N = 3$) in which the influence of the remaining modes of the system is disregarded; 2 – experimental case.

The influence of the voltage amplifier was considered in the results presented in Fig. 9. This means that $\hat{G}(s)$ and $G(s)$ from Eqs (25) and (24) were previously multiplied by the voltage amplifier gain ($g_a = 30V/V$). It is also important to mention that for the presented application: $K_c = 0.031472$ and $\omega_c = (\omega_3 + \omega_4)/2 = 145.33$ Hz.

It can be concluded from Fig. 9 that the numerical model must include the effect of the dynamical responses of higher order modes. However, some part of the results presented in Fig. 9, such as those in the range from 0 to 10 Hz, show that the results from Eq. (24) seem to be better. In the author's opinion this behavior come from other unknown effects, such as the characteristics of the bounding layer of the piezoelectric patches. This particular influence will be discussed later on this paper.

Finally, it can be added that the numerical model used is accurate enough to furnish a good representation of the dynamical system in the frequency range analyzed. Figure 10 presents a comparison between the case for which 150 modes are considered as in Eq. (24) and the case for which the higher order modes are taken into account according to Eq. (25). It can be observed in Fig. 10 that the two models are very close.

Another important aspect that can be observed in Fig. 9 is that the experimental transfer function differs from the numerical model. Besides, an accurate dynamic model of a flexible structure containing piezoelectric actuators and sensors is difficult to obtain, due to the unknown properties of the bonding layer material [6] discussed the influence and presented the formulation of a finite bonding layer in a flexible beam type structure. In the present work, a simpler model – that of a perfectly bonded piezoelectric – was used (Sec-

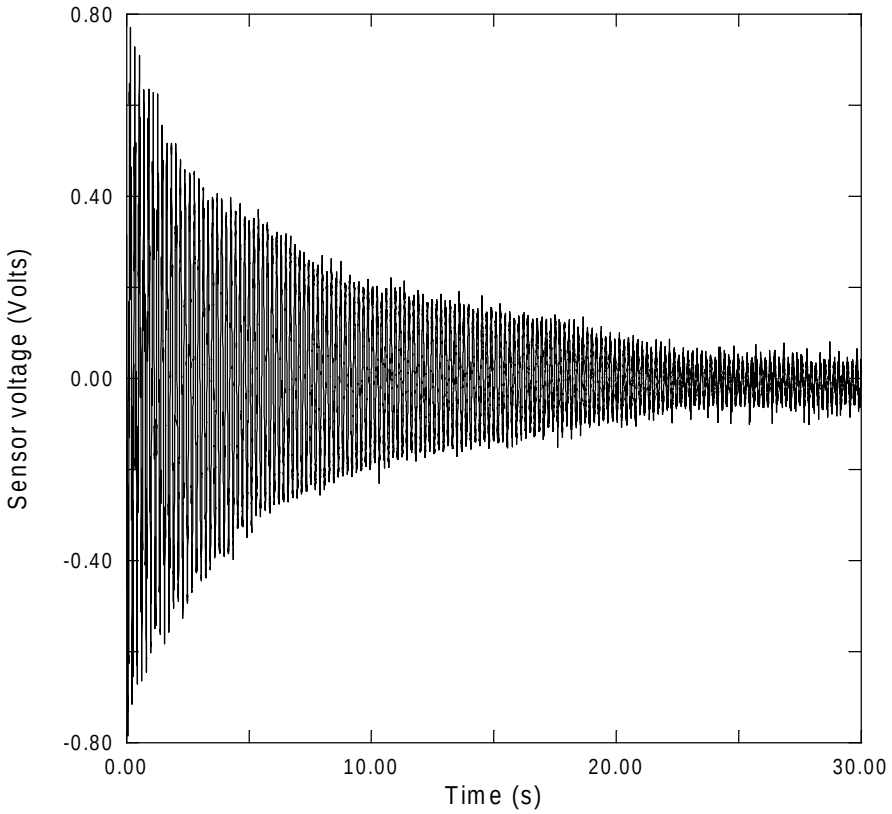

Fig. 13. Open-loop response of the experimental beam.

tion 2.1). However, the adhesive (bonding layer) modify the interface properties (damping and stiffness) between the piezoelectric element and the flexible structure. Therefore, a model adjusting technique (curve fitting) to determine the elastic modulus of the piezoelectric actuator bonding layer (E_a) was used. Then, the experimental and numerical transfer functions were used together in the following error expression to be minimized:

$$E(\omega) = \sum_{i=1}^{n} (\hat{G}(\omega_i) - G_{\exp}(\omega_i))^2 \tag{41}$$

were $\hat{G}(\omega)$ and $G_{\exp}(\omega)$ are the numerical and experimental transfer functions.

A classical optimization method (from the Optimization Toolbox for Matlab) was used to minimize $E(\omega)$. The optimal value for the elastic modulus of the piezoelectric material bonding layer was found to be $E_a = 25$ [GPa].

It should be pointed out that the adjusted value for the piezoelectric bonding layer modulus of elasticity is about 50% of the value specified in Table 1. The obvious consequence is that the actuator efficiency is reduced when it is bonded to the structure.

Figure 11 shows the transfer functions corresponding to the experimental and adjusted models.

8. Experimental evaluation of the optimal control performance

To analyze the performance of the LQG controller, an experimental verification was conducted, as shown schematically by Fig. 12.

The controller was implemented by using a dSpace DS1104 rapid prototyping controller board together with the Matlab and Simulink Software. The flexible beam was excited by using a shaker localized next to the clamp point. The electromechanical exciter was driven by a noise signal (0–100 Hz). A high voltage amplifier (capable of driving highly capacitive loads) was used to supply the necessary voltage to the actuating piezoelectric patch. Since the output voltage of the interface board is limited to $\pm 5\,[V]$, a voltage amplifier

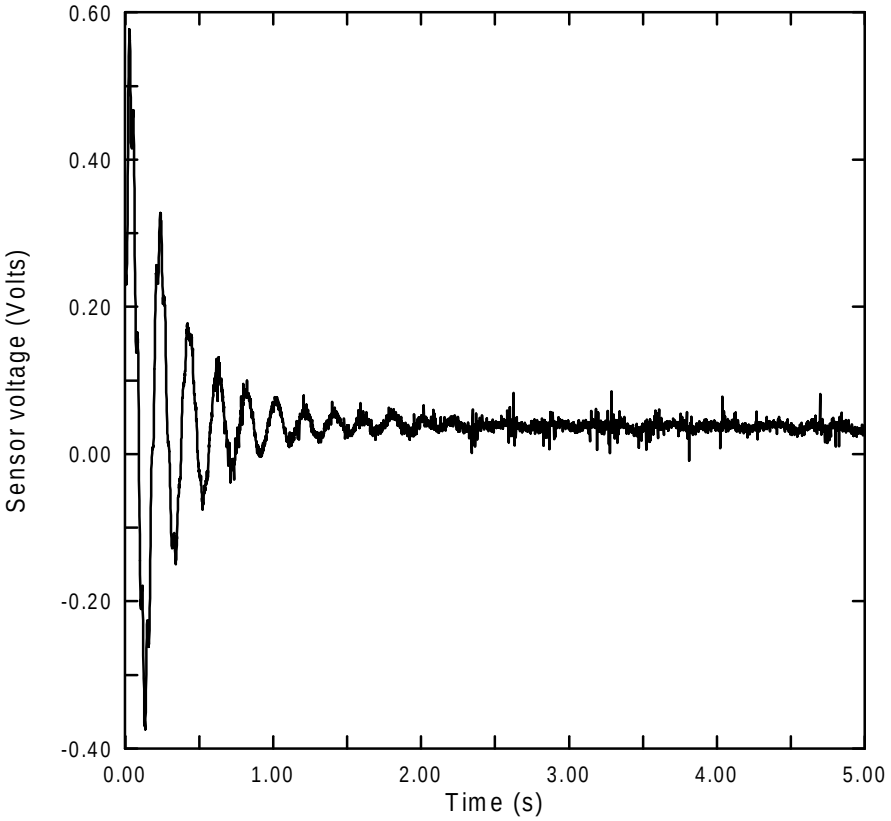

Fig. 14. Closed-loop sensor voltage response of the beam.

is needed to drive the actuator in the range of $\pm 150\,[V]$ for effective control performance.

In this case, the observability O and controllability C_o matrices:

$$O = ([C]\ [C][A] \ldots [C][A^{n-1}]) \tag{42}$$

$$C_o = ([B]\ [A][B] \ldots [A^{n-1}][B]) \tag{43}$$

have rank $2N$, where N is equal to 3. Then, the control design is carried out by using the iterative LQG algorithm with the following state weight matrices:

$$Q = \begin{bmatrix} \Omega & 0 \\ 0 & \Omega \end{bmatrix} \tag{44}$$

and

$$R = \gamma \tag{45}$$

where $\Omega = [1, \frac{\omega_1}{\omega_2}, \ldots, \frac{\omega_1}{\omega_N}]$, and $\gamma = 7.0 \times 10^{-6}$.

The control gain matrix $[G_c]$ (Eq. (31)) is then calculated for the maximum voltage applied to the piezo-actuator (150 V):

$$[G_c] = [-3.32 \times 10^2,\ -2.44 \times 10^3,\ -7.30 \times 10^3,\ 3.56 \times 10^2,\ 1.22 \times 10^2,\ 4.07 \times 10^1]$$

Using the following weight matrices:

$$Q_e = 10^{-7} I_{6\times 6} \tag{46}$$

and

$$R_e = 10^{-7} \tag{47}$$

Next step is to design a dynamic observer for the stability of the closed-loop system: $([A] - [L][C])$. That can be obtained by treating $([A]^T, [C]^T)$ as if they were $([A], [B])$ in the feedback control law design. The optimal observer gains are given as follows:

$$[L] = [6.6 \times 10^{-5},\ 6.97 \times 10^{-5},\ 5.75 \times 10^{-5},\ -9.18 \times 10^{-4},\ -2.62 \times 10^{-3},\ 2.46 \times 10^{-2}]^T$$

Then, the control signal (output voltage applied to the piezoelectric actuator) generated by the dSpace board

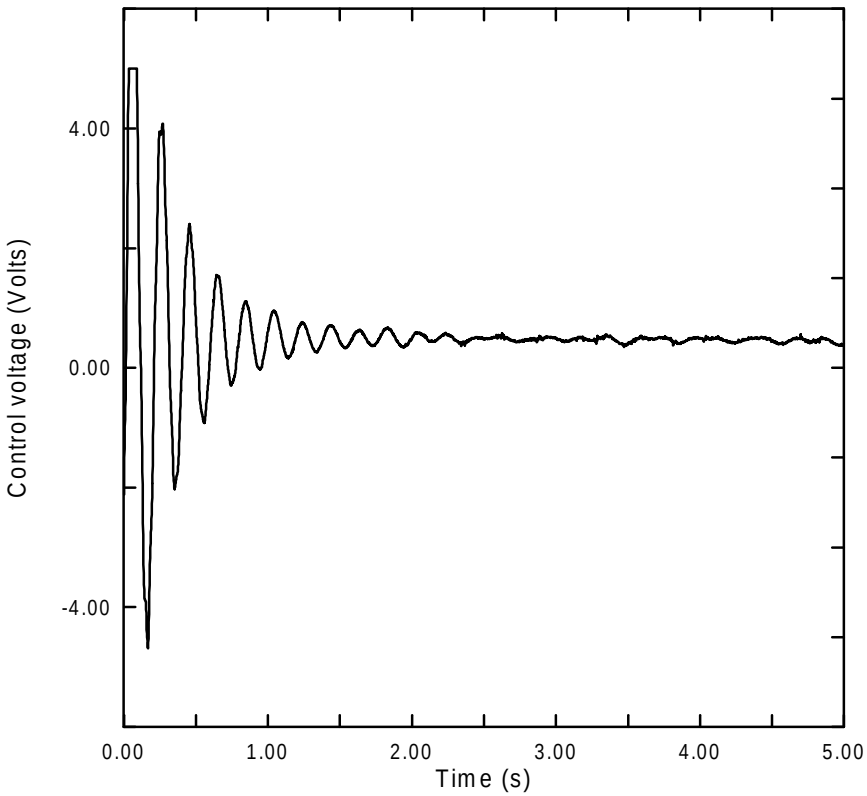

Fig. 15. Closed-loop control voltage response of the beam.

(the sampling frequency used was set to 1 KHz), is provided by $\{V_a(t)\} = -[G_c]\{\hat{q}(t)\}$ where $\{\hat{q}(t)\}$ (estimated state variables) is calculated by Eq. (33), where $V_s(t)$ is the voltage of the PVDF sensor.

The open-loop response of this flexible structure is obtained for an impulsive disturbance force generated by a hammer at the tip of the beam and the voltage output of the sensor $V_s(t)$ is shown in Fig. 13.

The active vibration control for the experimental case provides the sensor voltage output as shown by Fig. 14. Figure 15 presents the corresponding control voltage. Consequently, the flexible structure used in the experiments was stabilized by using the feedback control law (LQG).

Figure 16 compares the experimental transfer functions (magnitude and phase) of the open-loop and closed-loop systems (shaker signal to sensor voltage).

It can be observed that the control system was able to reduce the vibrations in the frequency range containing the first three modes. This corresponds to the maximum possible number of controlled modes for one sensor and one actuator, according to Eqs (42) and (43). The vibration reduction level was smaller for the third mode due to its corresponding weight element (see the weight matrix Ω – Eq. (44)). Figure 16 also shows the appearance of a torsion mode of the beam ($\approx$ 71 Hz). This problem can be overcome by substituting the electromechanical shaker by a PZT actuator.

9. Conclusions

An LQG controller was designed and implemented on a cantilever flexible beam containing a pair of piezoelectric sensor and actuator. A feed through term was added for minimizing the effect of the removed higher order modes in the low frequency range of the truncated model. The procedure used for placing sensors and actuators along the smart structure (modal cost technique) was proven to be effective. Besides, the modal cost technique has a strong intuitive appeal. It was observed that such a controller resulted in the reduction of the transverse vibration of the flexible structure. The controller was obtained by solving a standard optimal control problem for a finite-dimensional system. A number of experiments was performed, which demonstrated the effectiveness of the developed controller in reducing the vibrations of a flexible beam. It is impor-

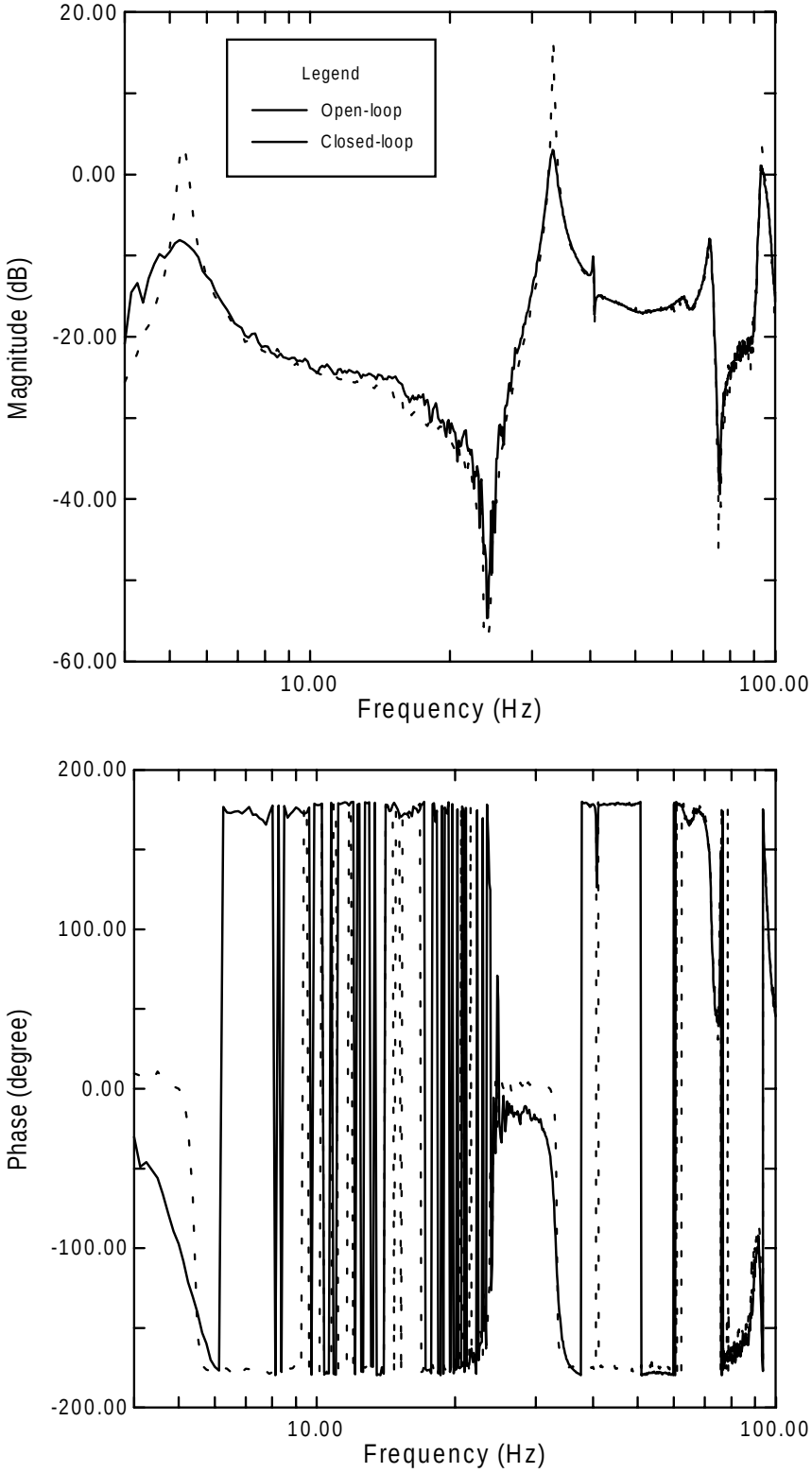

Fig. 16. Open and closed-loop transfer functions of the beam.

tant to say that the methodology presented in this paper can be extended to more sophisticated structures, such as thin plates.

Acknowledgement

The first author is thankful to Capes Foundation (Brazil) for his doctorate scholarship.

References

[1] J.J. Dosh, D.J. Inman and E. Garcia, A Self-sensing Piezoelectric Actuator for Collocated Control, *J. of Intell. Mater. Systems and Structures* **3**(1) (1992), 166–185.

[2] E.K. Dimitriadis, C.R. Fuller and C.A. Rogers, Piezoelectric Actuators for Distributed Vibration Excitation of Thin Plates, *Transactions of the ASME* **113** (1991), 100–107.

[3] C.R. Fuller, S.J. Elliott and P.A. Nelson, *Active Control of Vibration*, Academic Press Ltd, San Diego, CA, 1996, pp. 332.

[4] Moheimani, *Spatial Control for Active Vibration Control of Piezoelectric Laminates*, Proceedings of the 37th IEEE Conference on Decision & Control, Tampa, Flórida, 1998, pp. 4308–4313.

[5] H. Allik and T.J.R. Hughes, Finite Method for Piezoelectric Vibration, *International Journal for Numerical Methods in Engineering* **2** (1970), 151–157.

[6] E.F. Crawley and J. de Luis, Use of Piezoelectric Actuators as Elements of Intelligent Structures, *AIAA Journal* **10**(25) (1987), 1373–1385.

[7] H.S. Tzou and C.I. Tseng, Distributed Piezoelectric Sensor/Actuator Design for Dynamic Measurement/Control of Distributed Parameter Systems: A Piezoelectric Finite Element Approach, *Journal of Sound and Vibration* **138**(1) (1990), 17–34.

[8] L. Meirovitch, *Principles and Techniques of Vibrations*, Prentice-Hall, New Jersey, 1997.

[9] Y. Shen, A. Homaifar, M. Bikdash and D. Chen, *Genetic Algorithms and Fuzzy Based Vibration Control of Plate Using PZT Actuators*, Proceedings of the 37th IEEE Conference on Decision & Control, Tampa, Flórida, USA, 1998, pp. 2930–2933.

[10] Y. Shen, A. Homaifar, M. Bikdash and D. Chen, *Active Control of Flexible Structures Using Genetic Algorithms and LQG/LTR Approaches*, Proceedings of the American Control Conference, San Diego, California, USA, 1999, pp. 4398–4402.

[11] Z. Wang, S. Chen and W. Han, Integrated Structural and Control Optimization of Intelligent Structures, *Engineering Structures* **21** (1999), 183–191.

[12] G.C. Kirby and P. Matic, Optimal Actuator Size and Location Using Genetic Algorithms for Multivariable Control, *ASME Adaptive Structures and Composite Materials: Analysis and Application* **45** (1994), 325–335.

[13] C.E. Pereira and V. Steffen Jr., *Discrete-Continuous Optimization Techniques Applied to Smart Structure Vibration Control*, A Conference & Exposition on Structural Dynamics, Los Angeles, Califórnia, 2002.

[14] R.E. Skelton and A. Yousuff, Component Cost Analysis of Large Scale System, *International Journal of Control* **37**(2) (1983), 285–304.

[15] R.W. Soutas-Little and D.J. Inmam, *Engineering Mechanics*, Statics, Prentice-Hall, 1999.

[16] A. Baz and S. Poh, Performance of an Active Control System with Piezoelectric Actuators, *Journal of Sound and Vibrations* **126**(2) (1988), 327–343.

[17] A. Dimarogonas, *Vibration for Engineers*, Prentice Hall, Second Ed., New Jersey, 1996.

[18] H.R. Pota and T.E. Alberts, Multivariable Transfer Functions for a Slewing Piezoelectric Laminate Beam, *ASME Journal of Dynamic Systems, Measurement, and Control* **117** (1995), 353–359.

[19] N. Loix and A. Preumont, Remarks on the Modeling of Active Structures with Colocated Piezoelectric Actuators and Sensors, *Design Engineering Technical Conferences* **3** (1995), 335–339.

[20] Moheimani, *Minimizing the effect of out of bandwidth modes in the truncated assumed modes models of structures*, Proceedings of the American Control Conference, San Diego, CA, 1999, pp. 2718–2722.

[21] B.D.O. Anderson and J.B. Moore, *Optimal Control*, Linear Quadratic Methods, Prentice Hall, 1990.

[22] A.J. Laub, M.T. Heath, C.C. Paige and R.C. Ward, Computation of System Balancing Transformations and other Applications of Simultaneous Diagonalization Algorithms, *IEEE Transactions on Automatic Control* **32**(2), 115–122.

[23] R.E. Skelton, R. Singh and J. Ramakrishnan, *Component Model Reduction by Component Cost Analysis*, AIAA Guidance Navigation and Control Conference, Paper 88-4086, Mineapolis, MN, 1988.

[24] K. Ogata, *Modern Control Engineering*, 4th edition, Prentice Hall, 2001.

[25] ACX, Active Control eXperts, Inc. All rights reserved, 1996–2002, http://www.acx.com.

[26] D.J. Ewins, Modal Testing: Theory, Practice and Application (Mechanical Engineering Research Studies. Engineering Dynamics Series). Research Studies Press Ltd, 2000.